

SCT: A Simple Baseline for Parameter-Efficient Fine-Tuning via Salient Channels

Henry Hengyuan Zhao · Pichao Wang · Yuyang Zhao · Hao Luo · Fan Wang · Mike Zheng Shou

Received: date / Accepted: date

Abstract Pre-trained vision transformers have strong representation benefits to various downstream tasks. Recently, many parameter-efficient fine-tuning (PEFT) methods have been proposed, and their experiments demonstrate that tuning only 1% extra parameters could surpass full fine-tuning in low-data resource scenarios. However, these methods overlook the task-specific information when fine-tuning diverse downstream tasks. In this paper, we propose a simple yet effective method called “Salient Channel Tuning” (SCT) to leverage the task-specific information by forwarding the model with the task images to select partial channels in a feature map that enables us to tune only 1/8 channels leading to significantly lower parameter costs. Experiments outperform full fine-tuning on 18 out of 19 tasks in the VTAB-1K benchmark by adding only 0.11M parameters of the ViT-B, which is 780 \times fewer than its full fine-tuning counterpart. Fur-

Henry Hengyuan Zhao
Show Lab, National University of Singapore, Singapore
E-mail: hengyuan.z@u.nus.edu

Pichao Wang
Alibaba Group, USA
E-mail: pichaowang@gmail.com

Yuyang Zhao
National University of Singapore, Singapore
E-mail: yuyang.zhao@u.nus.edu

Hao Luo
Alibaba Group, China
E-mail: michuan.lh@alibaba-inc.com

Fan Wang
Alibaba Group, USA
E-mail: fan.w@alibaba-inc.com

Mike Zheng Shou (Corresponding author)
Show Lab, National University of Singapore, Singapore
E-mail: mike.zheng.shou@gmail.com

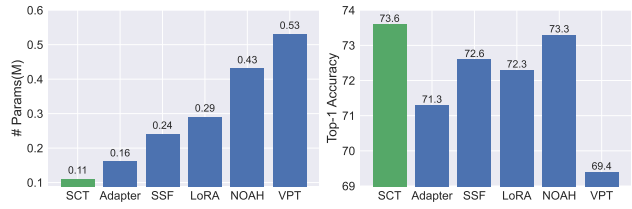


Fig. 1: The comparison of parameters and top-1 accuracy on VTAB-1K benchmark with different baselines. We only tune 96 channels in 768 channels of ViT-B/16, obtaining the best results compared with other methods.

thermore, experiments on domain generalization and few-shot learning surpass other PEFT methods with lower parameter costs, demonstrating our proposed tuning technique’s strong capability and effectiveness in the low-data regime. The code will be available at <https://github.com/showlab/SCT>

1 Introduction

Large vision transformers (ViT) have achieved remarkable success in computer vision tasks (Dosovitskiy et al., 2020; Liu et al., 2021; Yuan et al., 2022; Zhou et al., 2021a; Carion et al., 2020; Li et al., 2021; Strudel et al., 2021) by using large-scale training data, such as ImageNet21K and JFT-300M, to create strong representations. However, downstream recognition tasks often lack sufficient data to train from scratch. Therefore, transferring knowledge from pre-trained ViT models can significantly reduce training difficulty and produce promising results. End-to-end full fine-tuning is commonly used to inherit these robust representations, but

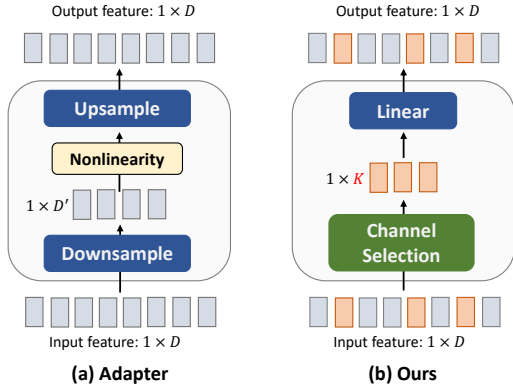


Fig. 2: Illustration of Adapter and our SCT. “Downsample” and “Upsample” represent the channel down-sampling and up-sampling operations. D represents the number of channel dimensions.

it faces two challenges. First, large models are prone to overfitting when tuning their massive weights on small downstream training data. Second, ViT models are too large to store all weights for each downstream task, making it infeasible to deploy fine-tuned models on resource-limited devices.

To mitigate the above two challenges, tuning a subset of parameters or adopting an external trainable module to preserve the knowledge learned from pre-trained models and adapt to the downstream tasks have been proposed. As for tuning a subset of full parameters, there are two common methods: tuning the classification head (Mahajan et al., 2018; Jia et al., 2021; Chen et al., 2021b) and bias term (Cai et al., 2020). Tuning the classification head freezes the weights of the backbone network and only updates the classification head, while tuning the bias term means unfreezing the bias term in the backbone network. Both methods lead to inferior performance.

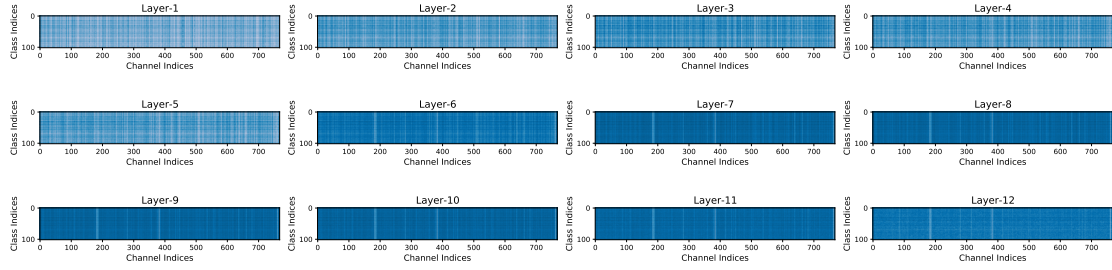
As for adopting an external trainable module, two lines of Parameter-Efficient Fine-Tuning (PEFT) methods are proposed. Firstly, adopt learnable prompts for each downstream task. VPT (Jia et al., 2022) is one representative method. One drawback of VPT is that its task-specific prompts are obtained through supervised learning, different from the text prompts used in NLP fields that users give. Another drawback is that it individually searches the prompt length for each task. It is not flexible in applying to a new task. Another direction (Chen et al., 2022b; Houlsby et al., 2019; Jie and Deng, 2022) is to add an adapter alongside the multi-head self-attention (MHSA) or MLP block in ViT (Dosovitskiy et al., 2020). Regardless of whether the structure of the adapter is MLP-like (Houlsby et al., 2019; Chen et al., 2022b) or Convolution-like (Jie and Deng, 2022),

these modules overlook leveraging the task-specific information in their efficient module, and the number of trainable parameters is not quite small and offers sub-optimal performance.

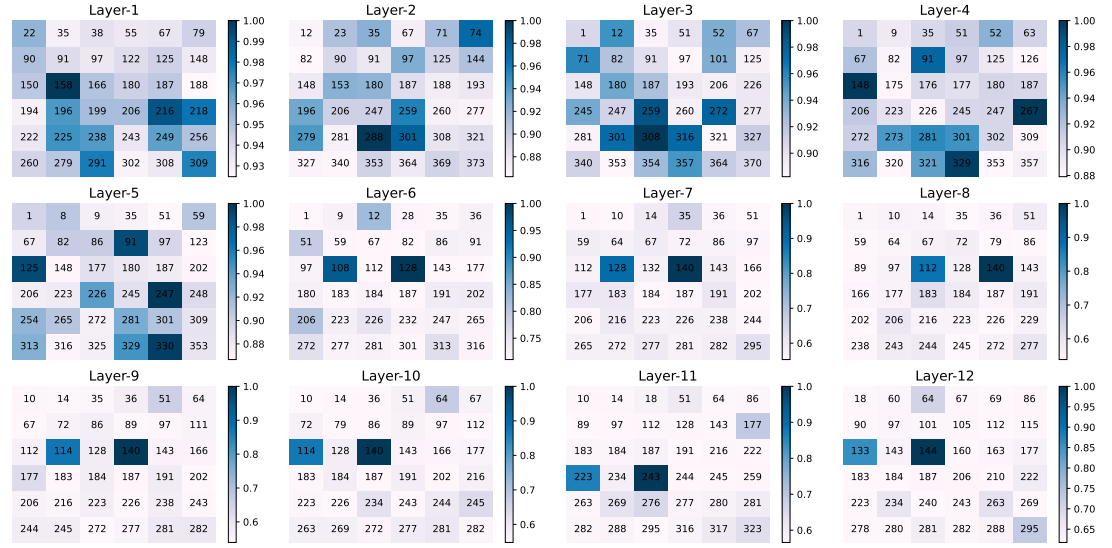
Though many works are proposed to explore the parameter-efficient tuning techniques, there still lacks the exploration of utilizing the task-specific information in the efficient module design as it is evident that channel bias exists in diverse downstream tasks (Luo et al., 2022). In this paper, we propose a simple and straightforward baseline that aims to find partial channels in the feature map by forwarding the pre-trained model with task-specific images. Such partial tuning enables us only fine-tune a small portion of channels which reduces the tunable parameters heavily. Our experiments surprisingly demonstrate that tuning only a small portion of task-specific channels is sufficient for downstream task adaptation in the low-data regime. As for selecting the task-specific channels, we propose the Class-Aware Importance Score (CAIS) by adopting L_2 norm as the criteria to evaluate the channel importance inspired by the classic pruning method (Han et al., 2015). We refer to the selected channels as “salient channels” (SC) since they have higher activation values and are crucial for task performance. This channel selection procedure helps to avoid the training costs by selecting the best structure as in NOAH (Zhang et al., 2022) or the best prompt length as in VPT (Jia et al., 2022). Compared with adapter-based methods (Houlsby et al., 2019; Chen et al., 2022b), selecting partial task-specific channels enables us to achieve lower parameter costs by removing the operations of “downsample” and “nonlinearity” as shown in Fig. 2. We conclude the contributions of our SCT as follows:

Contributions

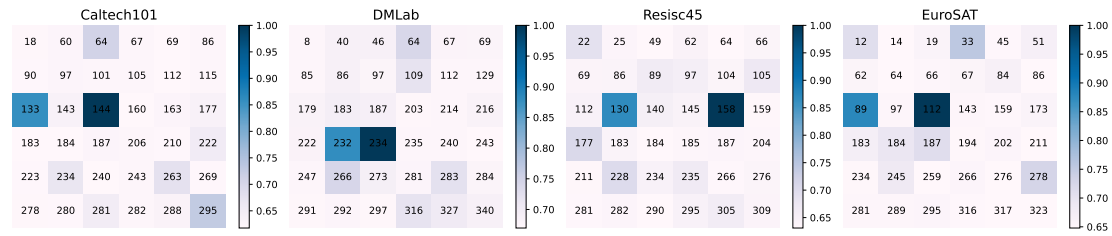
- We propose a simple baseline with the perspective in partial channel tuning (*i.e.*, salient channel tuning) for addressing the PEFT problem with leveraging task-specific information, achieving promising performance on 19 downstream tasks, domain generalization, and few-shot learning. The experiments demonstrate that tuning a subset of channels in a feature map efficiently for fine-tuning downstream tasks.
- It is the first time to reduce the extra parameters into 0.11M level of ViT-B with such competitive performance, which is 780 \times fewer parameters than the original model.
- Our proposed task-specific information storage baseline (SCT) offers a simple solution that requires minimal parameters while preventing the degradation of the original model in downstream domains



(a) Visualizations of the extracted feature maps on the *Caltech101* dataset at each transformer layer. Y-axis represents the class indices, and X-axis represents channel indices, *i.e.*, 768 in total. We categorize the total image features with the class label and then calculate each channel’s L_2 values. Thus, we obtain the 768 dimension vector for each class and find that some channels have higher activation values than others in all classes, as the vertical lines are shown in this figure.



(b) The top-36 selected salient channel indices on the *Caltech101* dataset at each transformer layer *i.e.*, Layer-1, Layer-2. Each layer selects different salient channels. As the layer goes deeper, the salient channels appear more concentrated. Darker color represents a larger activation value.



(c) We select the salient channels from the same layer on four downstream tasks. The results suggest that channel bias exists in various tasks.

Fig. 3: The visualizations of feature maps and the selected salient channel indices. All the results are obtained by ViT-B/16 pre-trained on ImageNet21K.

(full fine-tuning). The low parameter requirements and the ability to adapt with few samples make it a potential task knowledge storage unit for real-world applications.

2 Related Work

2.1 Vision Transformers

Transformer (Vaswani et al., 2017) has demonstrated outstanding results on natural language processing

and computer vision tasks. Lots of vision transformers (Chen et al., 2021a; d’Ascoli et al., 2021; Dong et al., 2022; Ali et al., 2021; Fan et al., 2021; Han et al., 2021; Rao et al., 2021; Yuan et al., 2021; Touvron et al., 2021; Liu et al., 2021; Wang et al., 2021; Zhou et al., 2021a) are proposed after the pioneering work ViT (Dosovitskiy et al., 2020). Many of them increase the model size gradually for state-of-the-art results and learn the rich representations by various architectural designs. Noteworthy, most of them are trained on the natural dataset and have the strong potential to be transferred to other domains/tasks. Adopting these models to the downstream tasks alleviates the training difficulty obviously and achieves promising results rapidly.

2.2 Parameter-Efficient Fine-Tuning Methods

PEFT focuses on adopting a trainable module with a few parameters for fine-tuning. Two lines of PEFT have been proposed recently. On the one hand, applying prompts (Jia et al., 2022; Liu et al., 2022; Xing et al., 2022; Zheng et al., 2022; Nie et al., 2022; Wang et al., 2022; Zhou et al., 2022a,b; Liao et al., 2023; Manli et al., 2022; Zhang et al., 2023b; Zang et al., 2022; Bar et al., 2022) to the backbone networks shows success on several vision tasks. VPT (Jia et al., 2022) first proposes the prompt-based method in computer vision fields. VPT injects the prompts into the transformer layer with a small number of extra parameters. However, one main limitation of VPT is that it relies on hand-crafted selection to determine the optimal prompt length for each task. This can be inflexible when applying the method to new tasks. Another limitation is that the task-specific prompts of VPT are obtained through the training procedure and cannot be given by the user as in the NLP field. In our work, to explicitly reduce the computations of searching the task-specific prompt length, we pass the training images into the backbone network and leverage the task-specific information by determining the salient channels. This procedure only needs one forward propagation without training costs.

On the other hand, adding a residual module (Houlsby et al., 2019; Chen et al., 2022b; Jie and Deng, 2022; Chen et al., 2022a) in the backbone networks also acquires promising results for performance and efficiency. Adapter (Houlsby et al., 2019), a widely used baseline in many tasks (Sung et al., 2022; Pan et al., 2022; Zhang et al., 2023a), proposes an MLP-like module, a successful design that first projects the original dimensional features into a smaller dimension with one nonlinear layer and projects it back to the original dimensions. It vastly reduces the number of parameters.

Inspired by its smallest intermediate dimensions, finding a small number of salient channels in a feature map might be enough for the adaptation. Unlike injecting trainable modules into the transformer blocks, LoRA (Hu et al., 2021) optimizes a low-rank decomposition matrix with a low intrinsic dimension to project the query, key, and value matrices used in multiheaded self-attention in ViT. As for NOAH (Zhang et al., 2022), a neural architecture search algorithm incorporates Adapter, LoRA, and VPT into its network search space. NOAH provides a strong baseline for performing consistently well on different datasets. SSF (Lian et al., 2022), a recently proposed strong baseline by only scaling and shifting the features to implement the efficient model tuning. Child-Tuning Xu et al. (2021) updates a subset of parameters of large pre-trained language models via strategically masking out the gradients of the non-child network during the backward process. AdaptFormer Chen et al. (2022b) is an adapter-like method. It explores the efficiency of the adapter-like architecture of vision transformers’ fine-tuning.

Unlike the above methods, our SCT handles the PEFT by leveraging the task-specific information and then proposes the Salient Channel Tuning Module (SCTM) from the new perspective of partial channel tuning, achieving low parameter costs and higher performance than previous methods.

3 Method

3.1 Not all channels are equal

To leverage task-specific information, this paper aims to find task-specific channels for fine-tuning. Here we provide a simple observation highlighting the “Salient Channels” that exist in the downstream tasks.

Previous works (Luo et al., 2017; Li et al., 2016; He et al., 2018; Liu et al., 2018; Han et al., 2015; Li et al., 2017) demonstrate that pruning some channels of deep neural networks has a marginal influence on the model performance but can significantly reduce the parameter number and computational cost. Such results reflect that the importance of different channels is not the same, *i.e.*, “Not all channels are equal”. Intuitively, the channel importance is different in terms of the tasks, which motivates us to investigate the impact of channel selection in model tuning.

To find task-specific channels, an intuitive way is to find some mutual channels across different categories. Thus, We first illustrate an observation between the pre-trained model and the downstream task. We choose *Caltech101* (Fei-Fei et al., 2004) (one of the downstream tasks from the VTAB-1K benchmark) as an example to

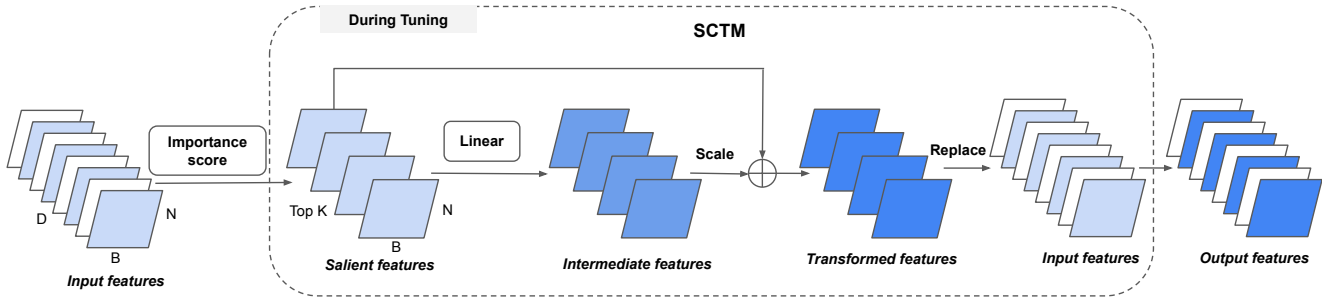


Fig. 4: The overview of proposed salient channel tuning module.

evaluate the intermediate features of each transformer layer of ViT. ViT-B pre-trained on ImageNet21K is the backbone, and we feed the whole dataset to extract the features between multi-head self-attention (“Attn”) and “MLP” blocks in all 12 transformer layers. Fig. 3 (a) shows some vertical lines in each subfigure of transformer layers. It indicates that when using a pre-trained model to extract the features on the target dataset, some channels have higher activation values than others, regardless of categories. We so-call these channels “salient channels”. To investigate the position of salient channels, we also report the index of selected top-36 salient channels after calculating the importance score of each layer in Fig. 3 (b). The number represents the channel index of the total of 768 channels. The darker color represents the higher activation values. We could find different layers have different salient channel sets. As the layer goes deeper, the salient channels appear more concentrated. We hypothesize that deeper layers contain more abstract information and information aggregated in a few channels. In contrast, the shallow layers extract more low-level representation, making the information dense.

It naturally raises a question: **Could we find salient channels in a feature map and then only tune these salient channels for efficient tuning?** To answer this question, we design a simple class-aware importance score to identify these salient channels and leverage a salient channel tuning module to tune these channels efficiently.

3.2 Class-Aware Importance Score

The selection of salient channels is crucial for the adaptation to downstream tasks, which should contain mutual information in all classes. Intuitively, we can directly use the mean feature of all the data samples to represent the downstream task distribution to determine the salient channels. However, considering downstream datasets may not always be balanced, treating

the whole dataset as a unity may be biased to the head classes, leading to the selected channels not representing the mutual information over all the classes. Consequently, we propose the Class-Aware Importance Score (CAIS), where the importance score calculation is conducted at each class and then averaged across all the classes. Assume the intermediate feature maps as $\{f_m^l \in \mathbb{R}^{B_m \times N \times D} | l, m \in \mathbb{N}, 1 \leq l \leq L \text{ and } 1 \leq m \leq M\}$, where the N and D represent the number of tokens and amount of channel dimension, respectively. L represents the total layers of the ViT backbone. The B_m is the volume of each class, and M represents the number of categories of the downstream recognition task. We first apply the L_2 norm regularization of each channel dimension of feature f_m^l :

$$\tilde{f}_m^l = \{\|f_{m,1}^l\|_2, \|f_{m,2}^l\|_2, \dots, \|f_{m,D}^l\|_2\}, \quad (1)$$

$$\|f_{m,i}^l\|_2 \in \mathbb{R}, \quad i \in \mathbb{N}, \quad 1 \leq i \leq D,$$

where $\tilde{f}_m^l \in \mathbb{R}^{1 \times D}$ is the importance score vector at l -th layer and m -th class. To investigate the salient channels, we average the $\tilde{f}_m^l \in \mathbb{R}^{1 \times D}$ over all classes to get the importance score at l -th layer:

$$Z^l = \frac{1}{M} \sum_{m=1}^M \tilde{f}_m^l, \quad \tilde{f}_m^l \in \mathbb{R}^{1 \times D}, \quad (2)$$

After getting the importance score vector $\{Z^l \in \mathbb{R}^{1 \times D} | l \in \mathbb{N}, 1 \leq l \leq L\}$, we can choose the largest K values of Z^l and then we can derive selected indices as $I^l = \text{topK}(Z^l)$, $I^l \in \mathbb{N}^{1 \times K}$ at l -th layer. Later, the salient channels at each layer are different across different downstream tasks, and it could explicitly involve task-specific information in the model fine-tuning. The procedures for selecting salient channels are shown in Algorithm 1.

3.3 Adapting ViT via Salient Channel Tuning

Given the importance score of selecting top- K salient channels, we propose a Salient Channel Tuning Mod-

ule (SCTM) in this paper. The overview of the SCTM is depicted in Fig. 4. Unlike other PEFT methods, our SCTM only contains a linear layer rather than an MLP-like adapter (Houlsby et al., 2019) involving two learnable layers and one activation layer illustrated in Fig. 2. Such a simple structure is easy to reproduce and maintains relatively low parameter costs. To inherit the original robust representations, we utilize a residual shortcut to fuse the salient features with intermediate features and use the $Scale \in \mathbb{R}$ (as shown in Fig. 4) to adjust the weights between both features, which is a constant parameter. After obtaining the transformed features, we insert the transformed features back into the input features at the same position. The unselected channels we keep frozen during fine-tuning. In Fig. 6, we present two forms of inserting the SCTM into the ViT. The “Ours-MLP” represents that we insert the SCTM after the MLP block, and the “Our-Attn” indicates that we put the SCTM after the MHSA block while before the MLP block. In the following experiments, “Ours-Attn” is the default injection position compared with other baselines.

Overall. Our SCT first feeds the training set to a backbone network to extract the intermediate features in different layers. Then, using the proposed CAIS to determine the salient channels and save the channel indices. During fine-tuning, we add our SCTM in each transformer layer and tune the selected channels with a linear layer while freezing other unselected channels.

Discussion. Firstly, different downstream tasks have their peculiarities, *i.e.*, “Not all channels are equal”. Previous PEFT methods (*i.e.*, Adapter) lack the consideration of explicitly using task-specific information. Instead, we propose the SCT explicitly leverage the task-specific information for channel selection, which could enable us to save the computations and extra parameters of the “Downsample” and “Nonlinearity” operations compared with Adapter (Houlsby et al., 2019). Secondly, calculating the salient channels offline could save the computations of searching the best prompt length (Jia et al., 2022) or the best network structure (Zhang et al., 2022). Thirdly, our results in Fig. 1 demonstrate that only adapting 12.5% channels could obtain competitive results compared to other baselines. Simultaneously, transforming a small portion of the features could significantly reduce the number of learnable parameters (e.g., $12 \times 96 \times 96$ is relatively more minor than the $12 \times 768 \times 768$). Fourthly, such a small amount of parameters largely reduces the difficulty of storing task-specific knowledge when we have many downstream tasks. To evaluate this simple baseline, we also test its few-shot capacity and domain generaliza-

Algorithm 1 The procedures of channel selection via class-aware importance score.

Inputs:

The pre-trained ViT model \mathcal{F} and the number of layers L ; The number of selected channels K and the total number of classes M ;

```

1: for each  $l \in [1, L]$  do
2:   Extract the feature  $f_m^l$  at each class  $m$ ;
3:   Apply the  $L_2$  norm regularization on each channel to
   obtain  $\tilde{f}_m^l$  via Eq. 1;
4:   Calculate the importance score  $Z^l$  of  $l$ -th layer via
   Eq. 2;
5:   Select top- $K$  largest channels  $I^l = \text{topK}(Z^l)$ ;
6: end for

```

Outputs: Selected channel indices of each transformer layer.

tion ability to meet the requirements of real-world applications.

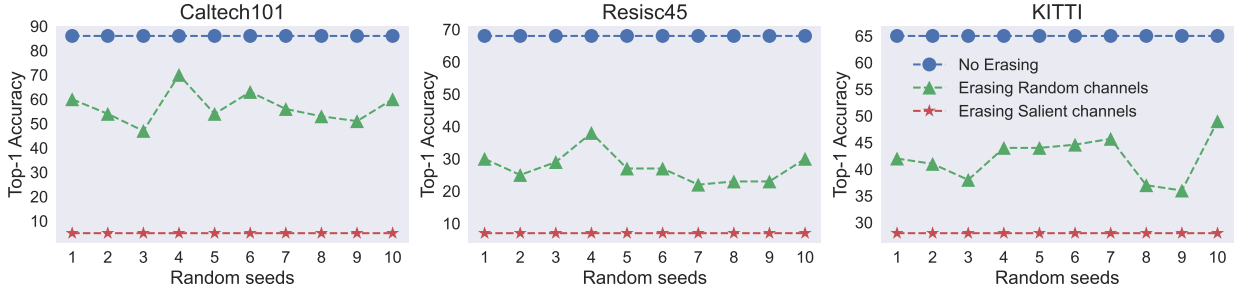
3.4 Channel Erasing Test

To assess the channel selection configuration, we give two toy tests to evaluate the effectiveness of salient channels as in Figure 5. The first test in Figure 5 (a) demonstrates the effectiveness of salient channels compared with random channel selection. The second test in Figure 5 (b) evaluates the importance of each layer. We erase the salient channels layer by layer. The curves suggest that for Natural type task Caltech101, the first four layers are more important than the last four layers as the accuracy drops significantly in the erasing first four layers. A similar trend is evident in the Resisc45 task. As for the KITTI task, the last four layers are as important as the first four.

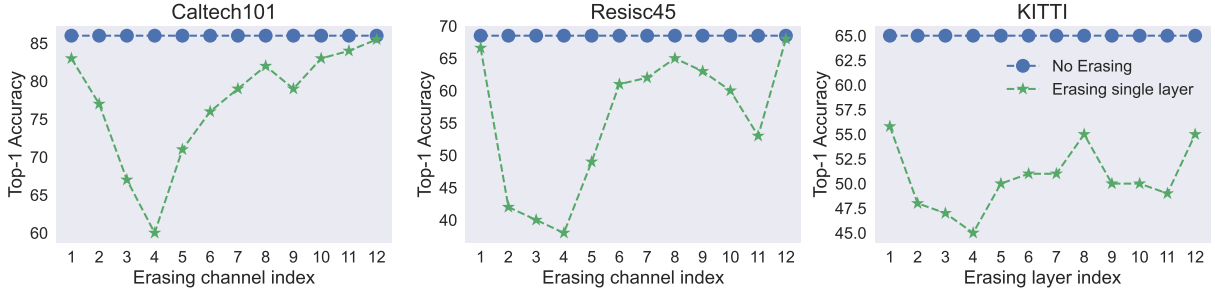
Based on the aforementioned tests, we manipulate the number of fine-tuned channels within the first four layers and the last eight layers, as outlined in Table 1. Increasing the number of fine-tuned channels within the first four layers (first and third rows) yielded enhancements of 0.1% for Caltech101 and 0.5% for KITTI, albeit with a 0.1% decline in Resisc45 performance. Notably, the influence of the last four layers on the final results is slight. Consequently, we explored the effect of decreasing the number of tuned channels within the last eight layers. The results (fourth and fifth rows) detailed in Table 1 indicate that reducing the K from 96 to 32 leads to a significant deterioration in performance. However, a slightly higher value compared with setting $K = 32$ across all 12 layers.

4 Experiments

This section compares our SCT with other state-of-the-art PEFT baselines on the VTAB-1K benchmark, using



(a) Evaluate the importance of salient channels on three datasets. We erase all layers with randomly selected channel indices and salient channel indices. To avoid the noise, we repeat the random selection process 10 times. The results demonstrate the effectiveness of our salient channel selection.



(b) We systematically remove one layer at a time, identified by its index. The resulting curve highlights the relative significance of the first four layers compared to the last four in the context of the Caltech101 and Resisc45 tasks. When considering the KITTI task, all layers are important for the final output.

Fig. 5: Channel erasing test.

Channel configurations	Caltech101	Resisc45	KITTI	Params
[96, 96, 96, 96, 96, 96, 96, 96, 96, 96, 96, 96, 96, 96, 96]	91.6	86.3	80.2	0.11M
[192, 192, 192, 192, 192, 192, 192, 192, 192, 192, 192, 192, 192, 192]	91.5	87.0	81.0	0.44M
[192, 192, 192, 192, 96, 96, 96, 96, 96, 96, 96, 96, 96, 96]	91.7	86.2	80.7	0.22M
[96, 96, 96, 96, 32, 32, 32, 32, 32, 32, 32, 32]	91.1	85.0	76.2	0.045M
[32, 32, 32, 32, 32, 32, 32, 32, 32, 32, 32, 32, 32]	90.3	84.8	74.0	0.01M

Table 1: Different number of fine-tuned channels on three tasks.

ViT and Swin Transformer backbones. In addition, we analyze the channel selection strategy, class-aware importance score, insert position, insert length, and the number of selected channels to verify SCT’s effectiveness further. Beyond evaluating performance on various downstream tasks, we also test SCT’s domain generalization capabilities using four datasets with natural distribution shifts and evaluate its performance in low-data regimes with five datasets in the few-shot scenario.

4.1 Training details

Following VPT (Jia et al., 2022), we utilize grid search to find the tuning-specific hyper-parameters, including learning rate and weight decay, based on the val set of each task as shown in Tab.2. For the hyper-parameter *Scale*, which is a manually defined constant to balance

the weight of transformed features and salient features, we search it at the range {0.1, 0.2, 0.3, 0.4, 0.5, 0.6, 0.7, 0.8, 0.9, 1.0}. During training, we use a standard image augmentation strategy: normalize with ImageNet means and standard deviation, randomly resize crop to 224×224, and random horizontal flip as in VPT.

4.2 Experiments on VTAB-1K Benchmark

Dataset. VTAB-1K (Zhai et al., 2019) contains 19 visual classification tasks which cover a broad spectrum of domains and semantics in three groups, *i.e.*, *Natural*, *Specialized*, and *Structured*. The *Natural* group contains 7 classic classification datasets of natural images. The *Specialized* group involves 4 datasets of two special scenarios: medical and remote-sensing. The *Structured* group has 8 datasets, mainly focusing on understand-

VTAB-1K, Domain Generalization, and Few-shot Learning	
Optimizer	AdamW (Loshchilov and Hutter, 2017)
$base_lr$ range	{0.1, 0.5, 0.01, 0.05, 0.001, 0.005, 0.0001, 0.0005}
Weight decay range	{0.1, 0.01, 0.05, 0.001, 0.005, 0.0005, 0.0001}
Learning rate schedule	cosine decay
Warm up epochs	10
Total epochs	100
Batch size	64

Table 2: Training details on each visual task with ViT-B/16.

Dataset	# Classes	Train	Val	Test
VTAB-1K (Zhai et al., 2019)				
Natural	CIFAR100 (Krizhevsky et al., 2009)	100		10,000
	Caltech101 (Fei-Fei et al., 2004)	102		6,048
	DTD (Cimpoi et al., 2014)	47		1,880
	Oxford-Flowers102 (Nilsback and Zisserman, 2006)	192	800/1000	200
	Oxford-PetS (Parkhi et al., 2012)	37		3,669
	SVHN (Netzer et al., 2011)	10		26,032
Specialized	Sun397 (Xiao et al., 2010)	397		21,750
	Patch Camelyon (Veeling et al., 2018)	2		32,768
	EuroSAT (Helber et al., 2019)	10	800/1000	200
	Resisc45 (Cheng et al., 2017)	45		1,880
Structured	Retinopathy (Kaggle and EyePacs, 2015)	5		42,670
	Clevr/count (Johnson et al., 2017)	8		15,000
	Clevr/distance (Johnson et al., 2017)	6		15,000
	DMLab (Beattie et al., 2016)	6		22,735
	KITTI-Dist (Geiger et al., 2013)	4	800/1000	200
	dSprites/location (Matthey et al., 2017)	16		711
	dSprites/orientation (Matthey et al., 2017)	16		73,728
	SmallNORB/azimuth (LeCun et al., 2004)	18		12,150
	SmallNORB/elevation (LeCun et al., 2004)	18		12,150
Domain generalization				
ImageNet	ImageNet-1K (Deng et al., 2009)	1,000	16 per class	50,000
	ImageNet-V2 (Recht et al., 2019)	1,000	N/A	N/A
	ImageNet-Sketch (Wang et al., 2019)	1,000	N/A	50,889
	ImageNet-A (Hendrycks et al., 2021b)	200	N/A	N/A
	ImageNet-R (Hendrycks et al., 2021a)	200	N/A	30,000
Few-shot Learning				
Few-shot	Food101 (Bossard et al., 2014)	101		20,200
	Stanford Cars (Krause et al., 2013)	196		1,635
	Oxford-Flowers102 (Nilsback and Zisserman, 2006)	102	1/2/4/8/16 per class	1,633
	FGVC-Aircraft (Maji et al., 2013)	100		3,333
	Oxford-Pets (Parkhi et al., 2012)	37		736

Table 3: Specifications of used datasets on VTAB-1K benchmark, Domain Generalization, and Few-shot Learning.

ing the structure of a scene, such as object counting and depth prediction. Each task of VTAB-1K contains 1000 training images. More details are available in Tab.3. Following [Zhang et al. \(2022\)](#); [Jia et al. \(2022\)](#), we use the 800-200 TRAIN-VAL split to determine the hyperparameters and the entire 1000 training data to train the final model. We report the average top-1 accuracy on the TEST set.

Baselines. We compare our method with three baselines **Full fine-tuning**, **Linear**, and **Bias** without external parameters and four baselines **Adapter** ([Houlsby et al., 2019](#)), **LoRA** ([Hu et al.,](#)

[2021](#)), **VPT** ([Jia et al., 2022](#)), and **NOAH** ([Zhang et al., 2022](#)) with external parameters. **Bias** method only updates all the bias terms in the pre-trained backbone. **Adapter** injects an additional MLP module into each transformer layer. **LoRA** adopts an optimized low-rank matrix to the MHSA module in the transformer layers. **VPT** is a visual prompt algorithm to incorporate the prompts with tokens into the backbone. **NOAH** is a neural architecture search algorithm incorporating the Adapter, LoRA, and VPT into the network search. **SSF** propose two learnable factors to scale and shift the features when fine-tuning the downstream

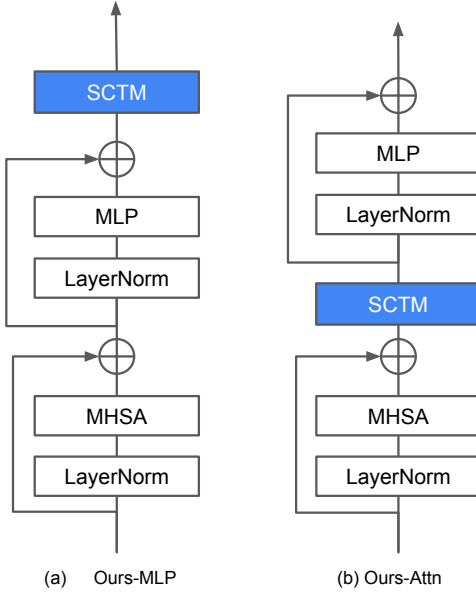


Fig. 6: Two types of structures when inserting SCTM into the backbone. Only SCTM is trainable, and other modules are frozen.

tasks. **AdaptFormer** proposes an adapter-like architecture for vision tasks. We directly use their released results or run their code to generate them to provide a fair comparison.

Performance with ViT backbone. We compare our SCT with the above 7 baselines in Tab. 4 and Fig. 7. We use ViT-B/16 as the backbone and insert SCTM in each transformer layer. The default K is set to 96, 1/8 of the total channels, leading to the trainable parameter number being only 0.11M. **First**, our SCT achieves the average accuracy of 73.6% on the 19 datasets, outperforming the full fine-tuning (85.8M) on 18 out of 19 datasets and gains the improvement of 6.3%, 2.5%, and 12.3% in the three groups, respectively, with only additional 0.13% of the backbone parameters. Such results reflect that SCT can greatly reduce the storage space and alleviate the overfitting problem common in fine-tuning large models. **Second**, compared with Adapter (0.16M) (Houlsby et al., 2019) that treats all the channels equally, selecting a part of salient channels for each downstream task is more effective and efficient, outperforming it by 2.3% in average accuracy. **Third**, compared with other PEFT methods, our SCT surpasses NOAH (0.43M) (Zhang et al., 2022) by 0.3% with only a quarter of its trainable parameters. When increasing the K to 192 with 0.44M extra parameters, our SCT surpasses NOAH (0.43) by 0.7 % average accuracy. Moreover, our SCT outperforms VPT (Jia et al., 2022) by 3.8%, 3.5%, and 4.9% in the three groups,

respectively. These results demonstrate that instead of specially designed structures for each downstream dataset, explicitly leveraging the task-specific information can reduce the computational cost in the model search and improve the performance. Moreover, compared with SSF (0.20M) (Lian et al., 2022) baseline, a method without an additional trainable module, our SCT only needs almost its half parameters and achieves an average improvement of 1.0% across 19 downstream tasks.

Performance with Swin Transformer Backbone. To verify the effectiveness of SCT with different backbones, we apply SCT on hierarchical transformers, *i.e.*, Swin-B. We use the same setting of inserting SCTM as in the ViT backbone: inserting the SCTM after the “Attn” block in the transformer layer. Considering deep layers contain more semantic information in the hierarchical structure, instead of applying SCTM on all the transformer layers, we insert it to the last half of the layers in the stage 3 and all layers of stage 4 of the Swin-B to keep a similar level of trainable parameters. The results of Tab. 5 show that SCT outperforms **full fine-tuning** in all 19 downstream tasks with only 0.12% parameters while other methods cannot. In addition, compared with the PEFT method, SCT outperforms VPT (Jia et al., 2022) by 5.9%, 3.0%, and 7.2% in the three groups, respectively. All the results above suggest that our SCT also applies to hierarchical transformers and can yield much more improvement than other PEFT methods.

4.3 Evaluation

Effectiveness of Salient Channel Tuning. We compare three channel selection strategies to verify the effectiveness of selecting salient channels in Tab. 6. The selection strategies include Salient Channel Selection (SC), Inconspicuous Channel Selection (IC), and Random Channel Selection (RC). IC selects channels with the lowest K values of L_2 norm, and RC denotes selecting K channels randomly. We randomly select three sets of channels (RC-1/2/3) for random channel selection to alleviate the outliers. As shown in Tab. 6, SC achieves the best results and outperforms IC by 2.4% in the average accuracy. Random channel selection could obtain better results than full fine-tuning, but all of them perform worse than SC. Interestingly, even IC can perform better than full fine-tuning, demonstrating that selecting a small subset of the channels can prevent the large model from overfitting to the small training set.

Effectiveness of Class-Aware Calculation for importance score. In Sec. 3.2, we introduced our method, which considers the impact of individual

# Params (M)	Natural						Specialized				Structured						Average				
	Cifar100	Caltech101	DTD	Flower102	Pets	SVHN	Sun397	Camelyon	EuroSAT	Resisc45	Retinopathy	Clevr-Count	Clevr-Dist	DMLab	KITTI-Dist	dSpr-Loc	dSpr-On	sNORB-Azim	sNORB-Ele		
Commonly used methods																					
Full	85.8	68.9	87.7	64.3	97.2	86.9	87.4	38.8	79.7	95.7	84.2	73.9	56.3	58.6	41.7	65.5	57.5	46.7	25.7	29.1	65.6
Linear	0	64.4	85.0	63.2	97.0	86.3	36.6	51.0	78.5	87.5	68.5	74.0	34.3	30.6	33.2	55.4	12.5	20.0	9.6	19.2	53.0
Bias	0.10	72.8	87.0	59.2	97.5	85.3	59.9	51.4	78.7	91.6	72.9	69.8	61.5	55.6	32.4	55.9	66.6	40.0	15.7	25.1	62.1
PEFT methods																					
VPT-Deep	0.53	78.8	90.8	65.8	98.0	88.3	78.1	49.6	81.8	96.1	83.4	68.4	68.5	60.0	46.5	72.8	73.6	47.9	32.9	37.8	69.4
NOAH	0.43	69.6	92.7	70.2	<u>99.1</u>	90.4	86.1	53.7	84.4	95.4	83.9	75.8	<u>82.8</u>	68.9	49.9	<u>81.7</u>	81.8	<u>48.3</u>	32.8	<u>44.2</u>	73.3
LoRA	0.29	67.1	91.4	69.4	98.8	90.4	85.3	54.0	<u>84.9</u>	95.3	84.4	73.6	82.9	69.2	49.8	78.5	75.7	47.1	31.0	44.0	72.3
Adapter-8 [†]	0.16	72.8	90.7	70.3	93.8	91.1	87.5	54.8	83.0	84.9	85.7	75.5	82.1	63.4	50.9	79.2	74.8	47.3	28.6	39.1	71.3
AdaptFormer-8 [†]	0.18	73.5	91.5	70.8	98.9	91.1	<u>87.8</u>	54.3	82.3	94.9	86.9	76.3	82.3	66.3	51.0	78.8	76.5	46.2	32.3	40.1	72.7
SCT	0.11	<u>75.3</u>	91.6	72.2	99.2	91.1	91.2	55.0	<u>85.0</u>	96.1	<u>86.3</u>	<u>76.2</u>	81.5	65.1	51.7	<u>80.2</u>	75.4	46.2	33.2	45.7	73.6

Table 4: Comparisons with state-of-the-art methods on the VTAB-1K benchmark with ViT-B/16. Average results are calculated across 19 datasets. “# Params” denotes the backbone’s average number of extra trainable parameters. The best performance and smallest parameter number are **bolded** in each column. Underline notes the second-best result. [†] means the model we implemented and trained on the same training setting, and the hyperparameters are selected by standard grid search since Adapter [Houlsby et al. \(2019\)](#) is a strong baseline for NLP tasks and Adaptformer [Chen et al. \(2022b\)](#) is not evaluated on VTAB-1K. The results of LoRA [Hu et al. \(2021\)](#) are from NOAH [Zhang et al. \(2022\)](#). The hidden dimensions of the Adapter and AdaptFormer are 8 and 96. The reduction dimension of LoRA we set is 8.

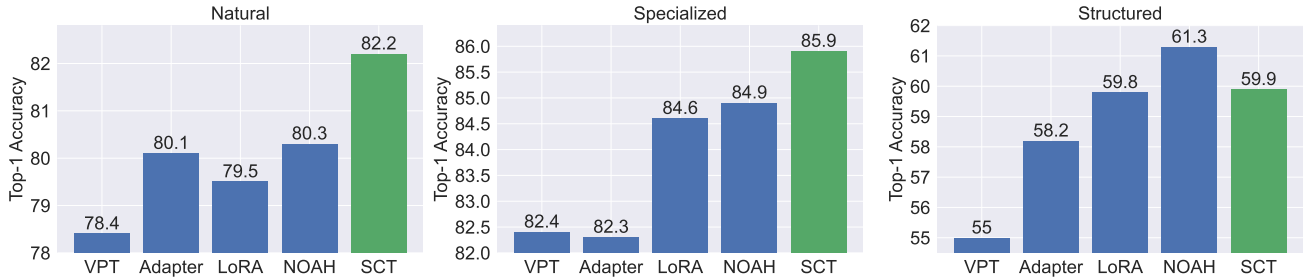


Fig. 7: Group-wise average results on VTAB-1K benchmark.

classes rather than treating the entire dataset as a whole when estimating the importance score (IS). This approach aims to identify the most significant channels based on the mutual information between categories and reduce the effects of imbalanced data. Our experimental results, presented in Tab. 7, demonstrate that adopting a class-aware calculation approach improves performance across all three groups.

Insert Position. As shown in Fig. 6, SCTM can be inserted after the MLP block (SCT_{MLP}) or between the MHSA block and MLP block (SCT_{Attn}). To investigate the influence of insert location, we compare two forms on the VTAB-1K benchmark in Tab. 8. Both achieve promising performances, and SCT_{Attn} outperforms SCT_{MLP} on two of the three groups. We conjecture that after gathering long-range dependencies with MHSA, the salient channels of features are more repre-

sentative, which can be better adapted to downstream tasks. We also evaluate the performance of inserting SCTM after both MHSA and MLP blocks, as shown in Tab. 10. Jointly inserting SCT_{Attn} and SCT_{MLP} only brings small improvements while the number of parameters doubles.

Number of insert depth. The insert depth is an important factor that can significantly influence the performance of a model. To investigate this, we conducted experiments by inserting SCTM into the last l layers of ViT-B and evaluated the performance on three representative tasks from each group of VTAB-1K. Our findings, presented in Fig. 9, reveal that increasing the insert depth results in a gradual improvement in performance. For the Resisc45 and DMLab tasks, we observed that competitive performance was achieved when the SCTM was inserted into the last six layers. Further

	# Params (M)	Natural										Specialized						Structured						Average
		Cifar100	Caltech101	DTD	Flower102	Pets	SVHN	Sun397	Camelyon	EuroSAT	Resisc45	Retinopathy	Clevr-Count	Clevr-Dist	DMLab	KITTI-Dist	dSpr-Loc	dSpr-Ori	sNORB-Azim	sNORB-Ele				
Commonly used methods																								
Full	86.7	72.2	88.0	71.4	98.3	89.5	90.1	45.0	86.6	96.9	87.7	79.4	75.7	59.8	54.6	78.6	79.4	53.6	34.6	40.9	74.2			
Linear	0	61.4	90.2	74.8	99.5	90.2	42.7	55.8	81.5	90.1	82.1	69.4	39.1	35.9	40.1	65.0	20.3	26.0	14.3	27.8	56.4			
Bias	0.24	73.0	86.8	65.6	97.7	87.5	56.4	52.3	80.4	91.6	76.1	72.5	47.3	48.5	34.7	66.2	57.6	36.2	34.7	66.2	62.1			
PEFT methods																								
VPT-Deep	0.19	79.6	90.8	78.0	99.5	91.4	42.3	51.7	84.9	96.2	85.0	72.0	67.6	59.4	50.1	61.3	74.4	50.6	25.7	25.7	68.6			
Adapter-8 [†]	0.11	74.2	90.7	75.9	99.5	92.5	38.0	55.6	88.2	95.0	88.9	76.9	71.4	56.7	54.1	84.5	79.6	35.8	21.9	35.3	69.2			
LoRA [†]	0.38	72.0	91.1	76.5	99.6	92.3	81.9	55.5	86.8	96.3	82.0	77.5	71.0	60.6	57.0	78.6	87.0	52.1	30.6	39.5	73.1			
AdaptFormer-8 [†]	0.13	74.6	91.0	76.2	99.6	92.4	83.5	55.4	87.0	95.2	88.9	76.8	73.8	57.9	54.8	82.7	82.2	49.7	21.6	36.9	72.6			
SSP [†]	0.27	75.4	90.0	75.1	91.0	91.2	92.3	55.0	88.8	84.2	89.1	76.8	71.0	53.5	56.0	83.4	84.2	52.8	30.5	33.2	72.3			
SCT (ours)	0.10	75.7	92.6	76.5	99.7	91.7	87.2	55.5	87.6	96.5	89.4	76.6	82.5	63.1	53.7	85.9	86.7	46.1	26.8	40.0	74.4			

Table 5: Per-task results on VTAB-1K benchmark with a pre-trained Swin-B. The average result is calculated on all 19 datasets in the VTAB-1K benchmark. The **Bold** text represents the best performance.

# Params (M)	Natural										Specialized						Structured						Average
	Cifar100	Caltech101	DTD	Flower102	Pets	SVHN	Sun397	Camelyon	EuroSAT	Resisc45	Retinopathy	Clevr-Count	Clevr-Dist	DMLab	KITTI-Dist	dSpr-Loc	dSpr-Ori	sNORB-Azim	sNORB-Ele				
Commonly used methods																							
Full	85.8	68.9	87.7	64.3	97.2	86.9	87.4	38.8	79.7	95.7	84.2	73.9	56.3	58.6	41.7	65.5	57.5	46.7	25.7	29.1	65.6		
Linear	0	64.4	85.0	63.2	97.0	86.3	36.6	51.0	78.5	87.5	68.5	74.0	34.3	30.6	33.2	55.4	12.5	20.0	9.6	19.2	53.0		
IC	0.11	68.8	91.5	71.5	99.0	91.1	89.0	54.3	85.3	95.8	86.6	75.2	78.1	61.2	50.3	79.0	73.1	40.0	27.4	36.7	71.1		
RC-1	0.11	72.1	90.4	71.7	99.1	91.2	90.2	54.0	84.2	95.5	85.7	75.9	78.8	62.5	49.5	77.6	72.2	43.3	27.3	40.9	71.7		
RC-2	0.11	74.1	91.4	72.1	99.2	90.9	90.2	55.1	83.0	95.7	86.3	75.0	79.3	62.5	50.4	78.2	72.5	43.2	28.1	39.8	72.0		
RC-3	0.11	71.3	91.1	70.9	99.0	90.9	89.6	54.4	83.9	95.7	85.9	74.8	78.6	62.2	48.9	80.2	71.2	42.1	27.8	38.5	71.4		
SCT	0.11	75.3	91.6	72.2	99.2	91.1	91.2	55.0	85.0	96.1	86.3	76.2	81.5	65.1	51.7	80.2	75.4	46.2	33.2	45.7	73.6		

Table 6: Per-task results on VTAB-1K benchmark with a pre-trained ViT-B/16. The average result is calculated on all 19 datasets in the VTAB-1K benchmark.

# Params (M)	Natural										Specialized						Structured						Average
	Cifar100	Caltech101	DTD	Flower102	Pets	SVHN	Sun397	Camelyon	EuroSAT	Resisc45	Retinopathy	Clevr-Count	Clevr-Dist	DMLab	KITTI-Dist	dSpr-Loc	dSpr-Ori	sNORB-Azim	sNORB-Ele				
Commonly used methods																							
Full	85.8	68.9	87.7	64.3	97.2	86.9	87.4	38.8	79.7	95.7	84.2	73.9	56.3	58.6	41.7	65.5	57.5	46.7	25.7	29.1	65.6		
Linear	0	64.4	85.0	63.2	97.0	86.3	36.6	51.0	78.5	87.5	68.5	74.0	34.3	30.6	33.2	55.4	12.5	20.0	9.6	19.2	53.0		
w/o CA	0.11	75.1	91.8	71.6	99.1	90.9	91.2	55.1	84.4	95.6	85.6	75.1	81.1	64.7	51.2	78.3	75.0	44.8	31.3	40.4	72.8		
w/ CA	0.11	75.3	91.6	72.2	99.2	91.1	91.2	55.0	85.0	96.1	86.3	76.2	81.5	65.1	51.7	80.2	75.4	46.2	33.2	45.7	73.6		

Table 7: Per-task results of evaluating the effectiveness of adopting the Class-Aware Importance Score. The average result is calculated on all 19 datasets in the VTAB-1K benchmark.

increases in the insert depth resulted in a plateau in performance, indicating that additional layers did not contribute significantly to the final performance.

Number of selected channels K . The most important hyperparameter of SCTM is the number of selected channels K , which influences the model architecture and the number of trainable parameters. **Note that** different from previous works (Jia et al., 2022; Zhang et al., 2022) that select hyperparameters for each

dataset, we use the same K for all the datasets. As shown in Tab.9, $\text{SCT}_{K=32}$ beats the full fine-tuning and bias tuning by 3.5% and 7.0%, respectively. Furthermore, $\text{SCT}_{K=32}$ only adopts 0.01M parameters while the tuning bias term adopts 0.10M. As shown in Fig. 8, the performance generally improves along with the increase of K . However, the improvement of $K = 192$ over $K = 96$ is marginal, while the number of parameters

	# Params (M)	Natural							Specialized				Structured							Average	
		Cifar100	Caltech101	DTD	Flower102	Pets	SVHN	Sun397	Camelyon	EuroSAT	Resisc45	Retiopathy	Clevr-Count	Clevr-Dist	DMLab	KITTI-Dist	dSpr-Loc	dSpr-Ori	sNORB-Azim	sNORB-Ele	
Full	85.8	68.9	87.7	64.3	97.2	86.9	87.4	38.8	79.7	95.7	84.2	73.9	56.3	58.6	41.7	65.5	57.5	46.7	25.7	29.1	65.6
Linear	0	64.4	85.0	63.2	97.0	86.3	36.6	51.0	78.5	87.5	68.5	74.0	34.3	30.6	33.2	55.4	12.5	20.0	9.6	19.2	53.0
SCT _{MLP}	0.11	72.9	92.0	71.6	99.1	90.6	90.5	54.9	86.2	95.9	85.9	76.0	81.3	64.7	50.7	78.9	77.2	43.3	29.3	43.6	72.9
SCT _{Attn}	0.11	75.3	91.6	72.2	99.2	91.1	91.2	55.0	85.0	96.1	86.3	76.2	81.5	65.1	51.7	80.2	75.4	46.2	33.2	45.7	73.6

Table 8: Per-task results of evaluating the effectiveness of the insert positions. The average result is calculated on all 19 datasets in the VTAB-1K benchmark.

	# Params (M)	Natural							Specialized				Structured							Average	
		Cifar100	Caltech101	DTD	Flower102	Pets	SVHN	Sun397	Camelyon	EuroSAT	Resisc45	Retiopathy	Clevr-Count	Clevr-Dist	DMLab	KITTI-Dist	dSpr-Loc	dSpr-Ori	sNORB-Azim	sNORB-Ele	
Full	85.8	68.9	87.7	64.3	97.2	86.9	87.4	38.8	79.7	95.7	84.2	73.9	56.3	58.6	41.7	65.5	57.5	46.7	25.7	29.1	65.6
Linear	0	64.4	85.0	63.2	97.0	86.3	36.6	51.0	78.5	87.5	68.5	74.0	34.3	30.6	33.2	55.4	12.5	20.0	9.6	19.2	53.0
Bias	0.10	72.8	87.0	59.2	97.5	85.3	59.9	51.4	78.7	91.6	72.9	69.8	61.5	55.6	32.4	55.9	66.6	40.0	15.7	25.1	62.1
SCT _{K=32}	0.01	71.7	90.3	70.2	99.0	90.1	85.8	53.1	82.2	95.6	84.8	75.7	71.6	62.1	48.3	74.0	59.1	42.0	24.5	33.6	69.1
SCT _{K=96}	0.11	75.3	91.6	72.2	99.2	91.1	91.2	55.0	85.0	96.1	86.3	76.2	81.5	65.1	51.7	80.2	75.4	46.2	33.2	45.7	73.6
SCT _{K=192}	0.44	76.0	91.5	72.3	99.1	91.2	92.2	55.2	86.2	95.7	87.0	76.1	82.5	64.0	52.1	81.0	75.5	47.5	34.7	45.6	74.0

Table 9: Per-task results of evaluating different K values on VTAB-1K benchmark.

	Cifar100	Resisc45	DMLab	Params
SCT _{Attn}	75.3	86.3	51.7	0.11M
SCT _{MLP}	72.9	85.9	50.9	0.11M
SCT _{Attn} + SCT _{MLP}	75.7	86.5	51.0	0.22M

Table 10: Comparison of different insert positions. The **Bold** text represents the best performance.

is four times larger. Considering both the effectiveness and efficiency, we set K to 96 by default.

4.4 Computation Analysis

Our analysis considers a ViT-B backbone with L layers and D dimensions and N tokens for a single image. We also assume that the intermediate dimension of Adapter (Houlsby et al., 2019) is D' , that the prompt length of VPT (Jia et al., 2022) is n , and that the total insert times of SSF (Lian et al., 2022) is m . Finally, we compare our proposed SCT approach to Adapter, VPT, and SSF in terms of parameters and FLOPs, as summarized in Tab. 12. Notably, our selection of K as $\frac{1}{8}D$ is fairly small compared to D . When the reduction ratio of the Adapter is also defined as 8, the parameters of the Adapter are $\frac{1}{4}LD^2$ while our parameters

are $\frac{1}{64}LD^2$. When we compare our approach to SSF, which inserts its module m times in the ViT-B backbone, the number of parameters for SSF is mLD . Examining the ViT-B backbone, we find that $m = 74$ and $\frac{1}{64}D = 12$, our parameters ($12LD < 74LD$) and FLOPs ($12NLD < 74NLD$) are smaller than SSF. Overall, our analysis suggests that SCT may offer PEFT a more efficient and effective baseline.

To assess the computational efficiency of our SCT approach, we choose to compare it with Adapter (0.16M) and SSF (0.20M) since they have a similar level of parameters and all of them are applied in the backbone network. We measured the running time and memory usage for both the training and testing phases using a batch size of 64 on the Cifar100 (VTAB-1K) dataset with the ViT-B backbone. We conducted training experiments on a single NVIDIA V100-32GB GPU and test experiments on a single NVIDIA A100-40GB GPU. As the usage of GPU memory during the training and testing phases is different. During the training phase, tensor activations, model parameters, gradients, and optimizer states (model, gradient, momentum) are the main sources. During the testing phase, tensor activations and model parameters are the main sources. Our results, as shown in Fig. 10, indicate that our SCT approach outperforms Adapter and SSF re-

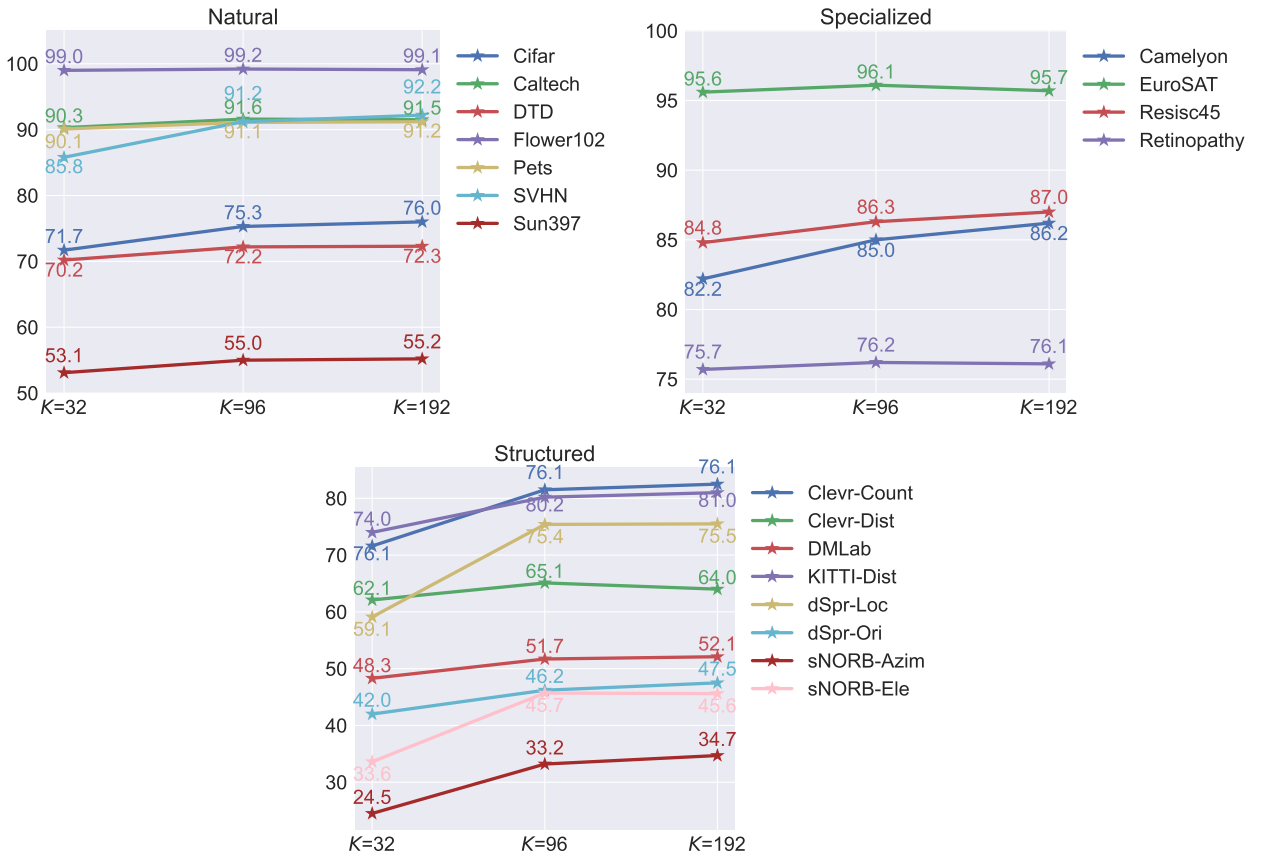
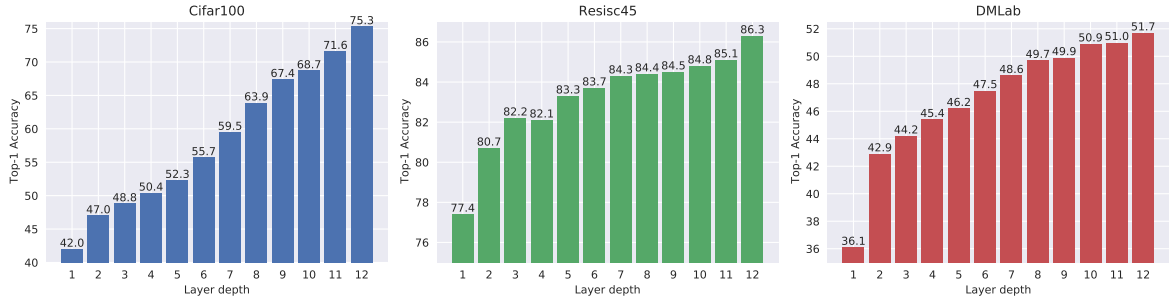
Fig. 8: Choosing different K values on 19 downstream tasks.

Fig. 9: Results of inserting SCTM into different layers. Zoom in for the best view.

garding training time and memory usage. As our tunable parameters are smaller than Adapter and SSF, the cost of gradients and optimizer states are small which helps us save the GPU memory during training. Specifically, our method requires only 12 additional SCT computations, while SSF requires 74 scaling and shifting operations. The training of SSF is not quite efficient compared with our SCT. However, during testing, the test time of our method is slightly higher than Adapter and SSF. Noted, SSF could merge its extra parameters to the original backbone with no extra inference costs while our method does not focus on reducing the com-

putation costs during inference. The reason for higher test costs compared with Adapter may be the extra operations of querying the salient channels from a full feature and then putting the projected salient channels back. Furthermore, we give exact test time cost results in Tab. 11. Here LoRA and SSF could merge its parameter into the backbone network thus we choose Full fine-tuning as the representative.

Methods	Test time	Memory	Params
Full fine-tuning	5.78 ms	336 MB	85.8 M
Adapter-8	6.87 ms	337 MB	85.8+0.16 M
AdaptFormer-8	7.88 ms	337 MB	85.8+0.18 M
SCT (Ours)	8.43 ms	337 MB	85.8+0.11 M

Table 11: We evaluate the test time for 1 image with resolution 224. We run 200 times and yield the average result.

	Adapter	VPT-Deep	SSF	TTC-Module
# Extra Parameters	$2LDD'$	nLD	mLD	LKK
# Extra FLOPs	$2NLDD'$	$2n(2N + n)LD$	$mNLDD$	$NLKK$

Table 12: A complexity analysis of Adapter (Houlsby et al., 2019), VPT (Jia et al., 2022), SSF (Lian et al., 2022), and our proposed TTC-Module.

4.5 Experiments on Domain Generalization

Dataset. In addition to evaluating the model on test data of the same distribution, modern deep neural networks commonly suffer from performance degradation when the testing distribution is different from that of the training set, *i.e.*, domain shift, which is inevitable in a real-world application. To alleviate this problem, domain generalization (Zhou et al., 2021b; Zhao et al., 2022; Zhou et al., 2022c; Yang et al., 2022a,b, 2021) is investigated in the community, aiming to train a model with one or multiple source domains that can perform well on other unseen target domains. To verify the generalization ability of our SCT, we follow Zhang et al. (2022) to conduct experiments on ImageNet and its variants. Specifically, we use the ImageNet-1K (Deng et al., 2009) as the source domain with 16-shot per category and evaluate our model on ImageNetV2 (Recht et al., 2019), ImageNet-Sketch (Wang et al., 2019), ImageNet-A (Hendrycks et al., 2021b), and ImageNet-R (Hendrycks et al., 2021a). ImageNetV2 (Recht et al., 2019) is collected from different sources from ImageNet-1K with the same protocol, and ImageNet-Sketch (Wang et al., 2019) contains the sketch images of ImageNet classes. Both of them use the same classes as ImageNet-1K. ImageNet-A (Hendrycks et al., 2021b) and ImageNet-R (Hendrycks et al., 2021a) contain the adversarially-filtered images and renditions of ImageNet data of a 200-class subset, respectively. We use a large version of SCT, *i.e.*, SCT-B, containing comparable parameters with NOAH (0.44M *vs.* 0.43M).

Results. In Tab. 13, we compare our SCT-B with Adapter (Houlsby et al., 2019), VPT (Jia et al., 2022), LoRA (Hu et al., 2021), and NOAH (Zhang et al., 2022) on the above datasets to verify the generalization ability. We can make two observations. **First**, SCT-B outperforms the previous best method (NOAH) on three of

the four target datasets and achieves comparable performance on ImageNetV2. Specifically, SCT-B yields an improvement of 2.5% on ImageNet-R over NOAH. **Second**, our SCT-B achieves an accuracy of 77.1% on the source domain, greatly outperforming previous methods by 6%. Since the backbone model is pre-trained on ImageNet-21K, the results on ImageNet-1K show that SCT can better enhance the knowledge transfer from superset to subset. The two observations demonstrate the superiority of our SCT over previous fine-tuning techniques on strong generalization ability.

4.6 Experiments on Few-shot Learning

Datasets. Following Zhang et al. (2022), we choose five fine-grained visual recognition datasets, including Food101 (Bossard et al., 2014), Flowers102 (Nilsback and Zisserman, 2006), StandfordCars (Krause et al., 2013), OxfordPets (Parkhi et al., 2012), and FGVCAircraft (Maji et al., 2013), to investigate the effectiveness of SCT in few-shot learning. The categories in these datasets cover various visual concepts closely related to our daily life: food, plant, vehicle, and animal. Next, we follow existing studies (Zhang et al., 2022; Jie and Deng, 2022) to evaluate our model under 1, 2, 4, 8, and 16 shots settings. The experimental setup is the same as in VTAB-1K.

Results. According to Fig. 11, our SCT surpasses other baselines in all settings in terms of average performance. In addition, SCT largely obtains the advantages at FGVCAircraft and OxfordPets datasets. For other datasets, SCT achieves competitive performance compared with other baselines. Such results demonstrate that SCT has a strong generalization ability that can be readily transferred to downstream tasks only with a few samples.

5 Conclusion

This paper introduces a simple baseline for PEFT, which is both simple and effective. Unlike previous methods, we adopt a channel selection perspective and propose a straightforward importance score to identify task-specific channels. By eliminating downsampling and nonlinearity operations, our method outperforms the similar Adapter method, requiring fewer parameters. We evaluate our algorithm on 19 downstream tasks and achieve the best results with only $780 \times$ fewer parameters than the original backbone. We also test our approach on four datasets with natural distribution shifts to assess domain generalization capabilities

	Source ImageNet	Target			
		-V2	-Sketch	-A	-R
Adapter (Houlsby et al., 2019)	70.5	59.1	16.4	5.5	22.1
VPT (Jia et al., 2022)	70.5	58.0	18.3	4.6	23.2
LoRA (Hu et al., 2021)	70.8	59.3	20.0	6.9	23.3
NOAH (Zhang et al., 2022)	71.5	66.1	24.8	11.9	28.5
SCT-B (ours)	77.1	65.8	28.5	12.1	31.0

Table 13: Comparison with previous methods on domain generalization. The backbone network is ViT-B/16. The number of salient channels is 192. The **Bold** text represents the best performance.

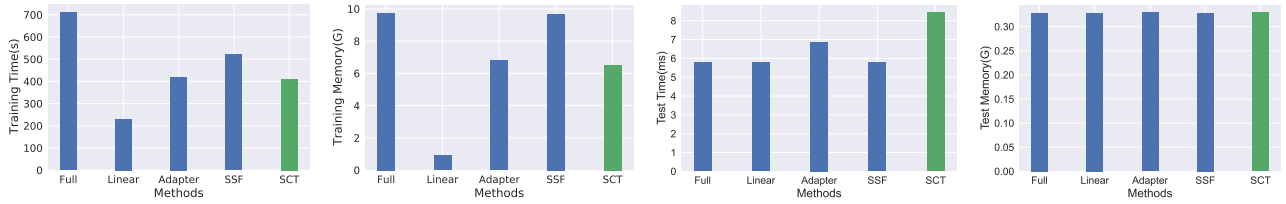


Fig. 10: The computational costs of training and test phases.

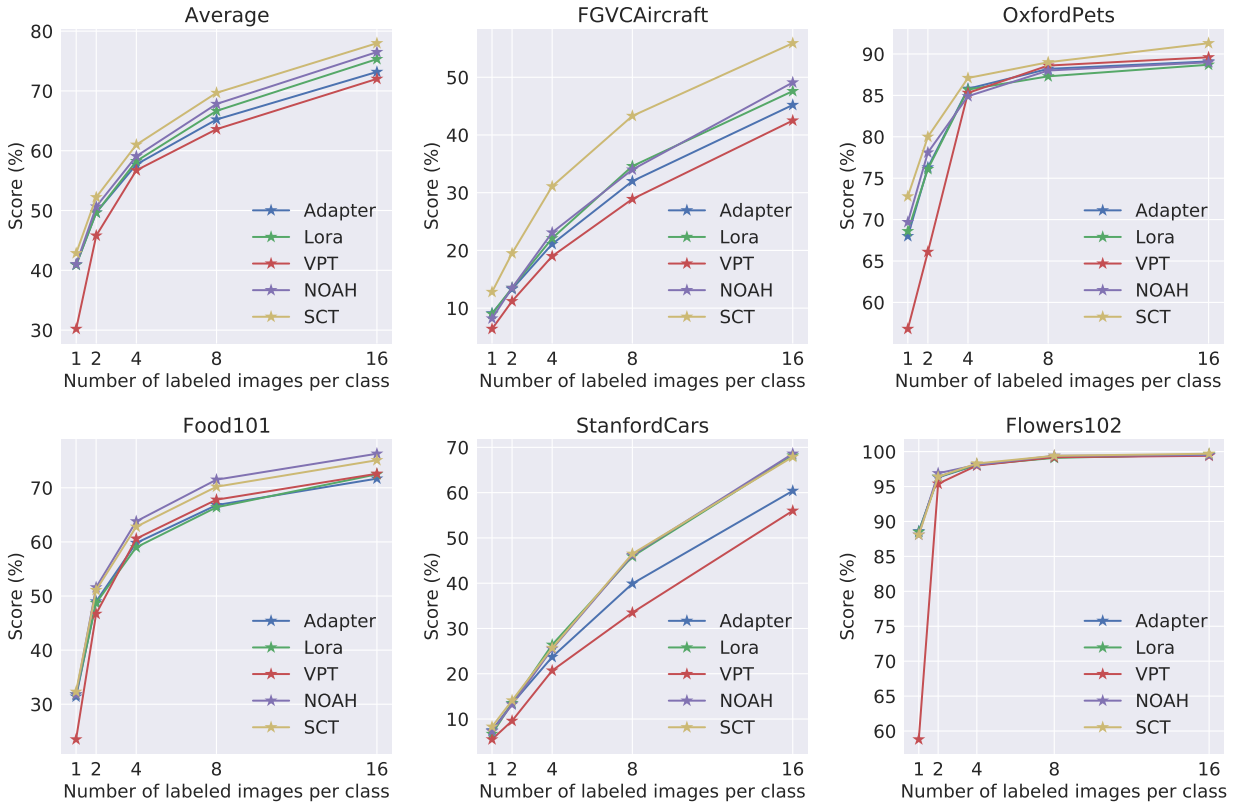


Fig. 11: Results of few-shot learning on five fine-grained visual recognition datasets.

and on five datasets in the few-shot scenario to evaluate performance in low-data regimes. Our approach is computationally efficient during both training and testing. Moreover, it is independent to prompt-based and

LoRa-like methods, allowing for further exploration in future research. Although our channel selection technique is straightforward, there is considerable potential to enhance its performance. Our baseline can be partic-

ularly useful in resource-limited situations as it requires fewer extra parameters and enables rapid adaptation to new tasks with just a few samples, making the simple and small modules effective knowledge storage units.

Acknowledgement

This research is supported by National Research Foundation, Singapore and A*STAR, under its RIE2020 Industry Alignment Fund – Industry Collaboration Projects (IAF-ICP) grant call (Grant No. I2001E0059) – SIA-NUS Digital Aviation Corp Lab. Mike Zheng Shou is supported by the National Research Foundation, Singapore, under its NRFF Award NRF-NRFF13-2021-0008, and Mike Zheng Shou's Start-Up Grant from NUS.

References

Ali A, Touvron H, Caron M, Bojanowski P, Douze M, Joulin A, Laptev I, Neverova N, Synnaeve G, Verbeek J, et al. (2021) Xcit: Cross-covariance image transformers. In: NeurIPS

Bar A, Gandelsman Y, Darrell T, Globerson A, Efros AA (2022) Visual prompting via image inpainting. arXiv preprint arXiv:220900647

Beattie C, Leibo JZ, Teplyashin D, Ward T, Wainwright M, Küttler H, Lefrancq A, Green S, Valdés V, Sadik A, et al. (2016) Deepmind lab. arXiv preprint arXiv:161203801

Bossard L, Guillaumin M, Gool LV (2014) Food-101-mining discriminative components with random forests. In: European conference on computer vision (ECCV), Springer, pp 446–461

Cai H, Gan C, Zhu L, Han S (2020) Tinytl: Reduce memory, not parameters for efficient on-device learning. In: NeurIPS

Carion N, Massa F, Synnaeve G, Usunier N, Kirillov A, Zagoruyko S (2020) End-to-end object detection with transformers. In: European conference on computer vision, Springer, pp 213–229

Chen CFR, Fan Q, Panda R (2021a) Crossvit: Cross-attention multi-scale vision transformer for image classification. In: Proceedings of the IEEE/CVF international conference on computer vision, pp 357–366

Chen H, Tao R, Zhang H, Wang Y, Ye W, Wang J, Hu G, Savvides M (2022a) Conv-adapter: Exploring parameter efficient transfer learning for convnets. arXiv preprint arXiv:220807463

Chen S, Ge C, Tong Z, Wang J, Song Y, Wang J, Luo P (2022b) Adaptformer: Adapting vision transformers for scalable visual recognition. arXiv preprint arXiv:220513535

Chen X, Xie S, He K (2021b) An empirical study of training self-supervised vision transformers. In: Proceedings of the IEEE/CVF International Conference on Computer Vision, pp 9640–9649

Cheng G, Han J, Lu X (2017) Remote sensing image scene classification: Benchmark and state of the art. Proceedings of the IEEE 105(10):1865–1883

Cimpoi M, Maji S, Kokkinos I, Mohamed S, , Vedaldi A (2014) Describing textures in the wild. In: Proceedings of the IEEE Conf. on Computer Vision and Pattern Recognition (CVPR)

Deng J, Dong W, Socher R, Li LJ, Li K, Fei-Fei L (2009) Imagenet: A large-scale hierarchical image database. In: Proceedings of the IEEE/CVF Conference on Computer Vision and Pattern Recognition (CVPR), Ieee, pp 248–255

Dong X, Bao J, Chen D, Zhang W, Yu N, Yuan L, Chen D, Guo B (2022) Cswin transformer: A general vision transformer backbone with cross-shaped windows. In: Proceedings of the IEEE/CVF Conference on Computer Vision and Pattern Recognition, pp 12124–12134

Dosovitskiy A, Beyer L, Kolesnikov A, Weissenborn D, Zhai X, Unterthiner T, Dehghani M, Minderer M, Heigold G, Gelly S, et al. (2020) An image is worth 16x16 words: Transformers for image recognition at scale. arXiv preprint arXiv:201011929

d’Ascoli S, Touvron H, Leavitt ML, Morcos AS, Biroli G, Sagun L (2021) Convit: Improving vision transformers with soft convolutional inductive biases. In: International Conference on Machine Learning, PMLR, pp 2286–2296

Fan H, Xiong B, Mangalam K, Li Y, Yan Z, Malik J, Feichtenhofer C (2021) Multiscale vision transformers. In: Proceedings of the IEEE/CVF International Conference on Computer Vision, pp 6824–6835

Fei-Fei L, Fergus R, Perona P (2004) Learning generative visual models from few training examples: An incremental bayesian approach tested on 101 object categories. In: conference on computer vision and pattern recognition workshop, IEEE, pp 178–178

Geiger A, Lenz P, Stiller C, Urtasun R (2013) Vision meets robotics: The kitti dataset. The International Journal of Robotics Research 32(11):1231–1237

Han K, Xiao A, Wu E, Guo J, Xu C, Wang Y (2021) Transformer in transformer. In: NeurIPS

Han S, Pool J, Tran J, Dally W (2015) Learning both weights and connections for efficient neural network. Advances in neural information processing systems 28

He Y, Kang G, Dong X, Fu Y, Yang Y (2018) Soft filter pruning for accelerating deep convolutional neural networks. In: IJCAI International Joint Conference on Artificial Intelligence

Helber P, Bischke B, Dengel A, Borth D (2019) Eurusat: A novel dataset and deep learning benchmark for land use and land cover classification. *IEEE Journal of Selected Topics in Applied Earth Observations and Remote Sensing* 12(7):2217–2226

Hendrycks D, Basart S, Mu N, Kadavath S, Wang F, Dorundo E, Desai R, Zhu T, Parajuli S, Guo M, et al. (2021a) The many faces of robustness: A critical analysis of out-of-distribution generalization. In: Proceedings of the IEEE/CVF International Conference on Computer Vision (ICCV), pp 8340–8349

Hendrycks D, Zhao K, Basart S, Steinhhardt J, Song D (2021b) Natural adversarial examples. In: Proceedings of the IEEE/CVF Conference on Computer Vision and Pattern Recognition (CVPR), pp 15262–15271

Houlsby N, Giurgiu A, Jastrzebski S, Morrone B, De Laroussilhe Q, Gesmundo A, Attariyan M, Gelly S (2019) Parameter-efficient transfer learning for nlp. In: International Conference on Machine Learning (ICML), PMLR, pp 2790–2799

Hu EJ, Shen Y, Wallis P, Allen-Zhu Z, Li Y, Wang S, Wang L, Chen W (2021) Lora: Low-rank adaptation of large language models. arXiv preprint arXiv:210609685

Jia M, Wu Z, Reiter A, Cardie C, Belongie S, Lim SN (2021) Exploring visual engagement signals for representation learning. In: Proceedings of the IEEE/CVF International Conference on Computer Vision, pp 4206–4217

Jia M, Tang L, Chen BC, Cardie C, Belongie S, Hariharan B, Lim SN (2022) Visual prompt tuning. In: ECCV

Jie S, Deng ZH (2022) Convolutional bypasses are better vision transformer adapters. arXiv preprint arXiv:220707039

Johnson J, Hariharan B, Van Der Maaten L, Fei-Fei L, Lawrence Zitnick C, Girshick R (2017) Clevr: A diagnostic dataset for compositional language and elementary visual reasoning. In: Proceedings of the IEEE/CVF Conference on Computer Vision and Pattern Recognition (CVPR), pp 2901–2910

Kaggle, EyePacs (2015) Kaggle diabetic retinopathy detection URL <https://www.kaggle.com/c/diabetic-retinopathy-detection/data>

Krause J, Stark M, Deng J, Fei-Fei L (2013) 3d object representations for fine-grained categorization. In: Proceedings of the IEEE international conference on computer vision workshops, pp 554–561

Krizhevsky A, Hinton G, et al. (2009) Learning multiple layers of features from tiny images

LeCun Y, Huang FJ, Bottou L (2004) Learning methods for generic object recognition with invariance to pose and lighting. In: Proceedings of the IEEE/CVF Conference on Computer Vision and Pattern Recognition (CVPR), IEEE, vol 2, pp II–104

Li H, Kadav A, Durdanovic I, Samet H, Graf HP (2016) Pruning filters for efficient convnets. arXiv preprint arXiv:160808710

Li H, Kadav A, Durdanovic I, Samet H, Graf HP (2017) Pruning filters for efficient convnets. In: International Conference on Learning Representations, URL <https://openreview.net/forum?id=rJqFGTslg>

Li Y, Xie S, Chen X, Dollar P, He K, Girshick R (2021) Benchmarking detection transfer learning with vision transformers. arXiv preprint arXiv:211111429

Lian D, Zhou D, Feng J, Wang X (2022) Scaling & shifting your features: A new baseline for efficient model tuning. In: Advances in Neural Information Processing Systems (NeurIPS)

Liao N, Shi B, Cao M, Zhang X, Tian Q, Yan J (2023) Rethinking visual prompt learning as masked visual token modeling. arXiv preprint arXiv:230304998

Liu L, Yu BX, Chang J, Tian Q, Chen CW (2022) Prompt-matched semantic segmentation. arXiv preprint arXiv:220810159

Liu Z, Sun M, Zhou T, Huang G, Darrell T (2018) Rethinking the value of network pruning. In: International Conference on Learning Representations

Liu Z, Lin Y, Cao Y, Hu H, Wei Y, Zhang Z, Lin S, Guo B (2021) Swin transformer: Hierarchical vision transformer using shifted windows. In: Proceedings of the IEEE/CVF International Conference on Computer Vision, pp 10012–10022

Loshchilov I, Hutter F (2017) Decoupled weight decay regularization. arXiv preprint arXiv:171105101

Luo JH, Wu J, Lin W (2017) Thinet: A filter level pruning method for deep neural network compression. In: Proceedings of the IEEE international conference on computer vision, pp 5058–5066

Luo X, Xu J, Xu Z (2022) Channel importance matters in few-shot image classification. In: International conference on machine learning, PMLR, pp 14542–14559

Mahajan D, Girshick R, Ramanathan V, He K, Paluri M, Li Y, Bharambe A, Van Der Maaten L (2018) Exploring the limits of weakly supervised pretraining. In: Proceedings of the European conference on computer vision (ECCV), pp 181–196

Maji S, Rahtu E, Kannala J, Blaschko M, Vedaldi A (2013) Fine-grained visual classification of aircraft. arXiv preprint arXiv:13065151

Manli S, Weili N, De-An H, Zhiding Y, Tom G, Anima A, Chaowei X (2022) Test-time prompt tuning for zero-shot generalization in vision-language models. In: NeurIPS

Matthey L, Higgins I, Hassabis D, Lerchner A (2017) dsprites: Disentanglement testing sprites dataset

Netzer Y, Wang T, Coates A, Bissacco A, Wu B, Ng AY (2011) Reading digits in natural images with unsupervised feature learning

Nie X, Ni B, Chang J, Meng G, Huo C, Zhang Z, Xiang S, Tian Q, Pan C (2022) Pro-tuning: Unified prompt tuning for vision tasks. arXiv preprint arXiv:220714381

Nilsback ME, Zisserman A (2006) A visual vocabulary for flower classification. In: Proceedings of the IEEE/CVF Conference on Computer Vision and Pattern Recognition (CVPR), IEEE, vol 2, pp 1447–1454

Pan J, Lin Z, Zhu X, Shao J, Li H (2022) St-adapter: Parameter-efficient image-to-video transfer learning. Advances in Neural Information Processing Systems 35:26462–26477

Parkhi OM, Vedaldi A, Zisserman A, Jawahar C (2012) Cats and dogs. In: Proceedings of the IEEE/CVF Conference on Computer Vision and Pattern Recognition (CVPR), IEEE, pp 3498–3505

Rao Y, Zhao W, Liu B, Lu J, Zhou J, Hsieh CJ (2021) Dynamicvit: Efficient vision transformers with dynamic token sparsification. In: NeurIPS

Recht B, Roelofs R, Schmidt L, Shankar V (2019) Do imagenet classifiers generalize to imagenet? In: International Conference on Machine Learning (ICML), PMLR, pp 5389–5400

Strudel R, Garcia R, Laptev I, Schmid C (2021) Segmerner: Transformer for semantic segmentation. In: Proceedings of the IEEE/CVF International Conference on Computer Vision, pp 7262–7272

Sung YL, Cho J, Bansal M (2022) Vl-adapter: Parameter-efficient transfer learning for vision-and-language tasks. In: Proceedings of the IEEE/CVF Conference on Computer Vision and Pattern Recognition, pp 5227–5237

Touvron H, Cord M, Sablayrolles A, Synnaeve G, Jégou H (2021) Going deeper with image transformers. In: Proceedings of the IEEE/CVF International Conference on Computer Vision, pp 32–42

Vaswani A, Shazeer N, Parmar N, Uszkoreit J, Jones L, Gomez AN, Kaiser L, Polosukhin I (2017) Attention is all you need. In: NeurIPS

Veeling BS, Linmans J, Winkens J, Cohen T, Welling M (2018) Rotation equivariant cnns for digital pathology. In: International Conference on Medical image computing and computer-assisted intervention, Springer, pp 210–218

Wang H, Ge S, Lipton Z, Xing EP (2019) Learning robust global representations by penalizing local predictive power. In: NeurIPS

Wang P, Wang X, Wang F, Lin M, Chang S, Xie W, Li H, Jin R (2021) Kv_t: k-nn attention for boosting vision transformers. arXiv preprint arXiv:210600515

Wang S, Chang J, Wang Z, Li H, Ouyang W, Tian Q (2022) Fine-grained retrieval prompt tuning. arXiv preprint arXiv:220714465

Xiao J, Hays J, Ehinger KA, Oliva A, Torralba A (2010) Sun database: Large-scale scene recognition from abbey to zoo. In: 2010 IEEE computer society conference on computer vision and pattern recognition, IEEE, pp 3485–3492

Xing Y, Wu Q, Cheng D, Zhang S, Liang G, Zhang Y (2022) Class-aware visual prompt tuning for vision-language pre-trained model. arXiv preprint arXiv:220808340

Xu R, Luo F, Zhang Z, Tan C, Chang B, Huang S, Huang F (2021) Raise a child in large language model: Towards effective and generalizable fine-tuning. In: Proceedings of the 2021 Conference on Empirical Methods in Natural Language Processing (EMNLP), Association for Computational Linguistics

Yang J, Zhou K, Li Y, Liu Z (2021) Generalized out-of-distribution detection: A survey. arXiv preprint arXiv:211011334

Yang J, Wang P, Zou D, Zhou Z, Ding K, Peng W, Wang H, Chen G, Li B, Sun Y, et al. (2022a) Openood: Benchmarking generalized out-of-distribution detection. arXiv preprint arXiv:221007242

Yang J, Zhou K, Liu Z (2022b) Full-spectrum out-of-distribution detection. arXiv preprint arXiv:220405306

Yuan L, Chen Y, Wang T, Yu W, Shi Y, Jiang ZH, Tay FE, Feng J, Yan S (2021) Tokens-to-token vit: Training vision transformers from scratch on imagenet. In: Proceedings of the IEEE/CVF International Conference on Computer Vision, pp 558–567

Yuan L, Hou Q, Jiang Z, Feng J, Yan S (2022) Volo: Vision outlooker for visual recognition. IEEE Transactions on Pattern Analysis and Machine Intelligence

Zang Y, Li W, Zhou K, Huang C, Loy CC (2022) Unified vision and language prompt learning. arXiv preprint arXiv:221007225

Zhai X, Puigcerver J, Kolesnikov A, Ruyssen P, Riquelme C, Lucic M, Djolonga J, Pinto AS, Neumann M, Dosovitskiy A, et al. (2019) A large-scale study of representation learning with the visual task adaptation benchmark. arXiv preprint arXiv:191004867

Zhang B, Jin X, Gong W, Xu K, Zhang Z, Wang P, Shen X, Feng J (2023a) Multimodal video adapter for parameter efficient video text retrieval. arXiv preprint arXiv:230107868

Zhang Y, Zhou K, Liu Z (2022) Neural prompt search. arXiv preprint arXiv:220604673

Zhang Y, Zhou K, Liu Z (2023b) What makes good examples for visual in-context learning?

Zhao Y, Zhong Z, Zhao N, Sebe N, Lee GH (2022) Style-hallucinated dual consistency learning for domain generalized semantic segmentation. In: ECCV

Zheng Z, Yue X, Wang K, You Y (2022) Prompt vision transformer for domain generalization. arXiv preprint arXiv:220808914

Zhou J, Wang P, Wang F, Liu Q, Li H, Jin R (2021a) Elsa: Enhanced local self-attention for vision transformer. arXiv preprint arXiv:211212786

Zhou K, Yang Y, Qiao Y, Xiang T (2021b) Domain generalization with mixstyle. In: ICLR

Zhou K, Yang J, Loy CC, Liu Z (2022a) Conditional prompt learning for vision-language models. In: IEEE/CVF Conference on Computer Vision and Pattern Recognition (CVPR)

Zhou K, Yang J, Loy CC, Liu Z (2022b) Learning to prompt for vision-language models. International Journal of Computer Vision (IJCV)

Zhou K, Zhang Y, Zang Y, Yang J, Loy CC, Liu Z (2022c) On-device domain generalization. arXiv preprint arXiv:220907521